MULTILAYER SnO_2:Sb TRANSPARENT ELECTRONIC CONDUCTING COATINGS MADE BY THE SOL-GEL PROCESS

G. Gasparro, D. Ganz, J. Pütz, M. A. Aegerter *

Institut für Neue Materialien - INM
Department of Coating Technology
Im Stadtwald, Gebäude 43
D-66123 Saarbrücken

ABSTRACT

Transparent conducting thin sol-gel SnO_2:Sb multilayer coatings having the same total thickness, but different numbers of layers have been deposited on borosilicate glass by the dip-coating method using an ethanolic solution of $SnCl_2(OAc)_2$ doped with 5 mol% $SbCl_3$. The densification of the multilayers was done by 3 different processes. In process I each layer was dried at 200°C and the coating process repeated to obtain a thick dry coating which was then sintered as a whole at 550°C. In process II every single layer was dried at 120°C and then directly sintered at 550°C before repeating the coating process. In process III every single layer was directly sintered at 550°C without a drying step. The electrical properties and the morphologies of the coatings depend highly on the sintering and drying conditions. With process I all layers are homogenous and have a high resistivity ($1.4x10^{-2}\Omega cm$) whatever their thickness. The multilayers produced by process II and III show a sandwich structure with alternated dense and porous layers. The resistivity of a 10 times dipped multilayers obtained by these processes is about $3,2x10^{-3}\Omega cm$. Moreover the electrical properties vary with the number of layers whereas in process I no such correlation can be found. A model was developed which allows to calculate the electrical properties of the dense and porous layers. The chemical composition of the homogeneous coating and of the multilayers with the alternated structure is also reported.

INTRODUCTION

Thin transparent conducting oxide coatings such as tin doped indium oxide (ITO), fluor or antimony doped tin dioxide (FTO, ATO) are of broad interest because of their high optical transmission, high conductivity and numerous of application fields [1]. They are used as electrodes in solar cells [2], LCD's, optical electrical devices [3], catalysts or as heat shields [4]. Commercial coatings are essentially made by physical or chemical deposition techniques like sputtering [5], spray pyrolysis [2] or chemical vapour deposition (CVD) [6]. The vacuum techniques give coatings with good electrical and optical quality but bear the disadvantage of high production costs. The spray techniques are cheaper and give also highly conductive coatings but with lower homogeneity.

The sol-gel technique [7-15] allows to produce layers with high transmission in the visible part but their resistivity was always found at least one order of magnitude higher than those obtained for coatings prepared by the other methods. Therefore numerous investigations are underway to understand the reasons of this high resistivity and to improve the electrical properties of sol-gel coatings. The morphology of the sol-gel layer is one of the main factor influencing the conductivity of the layer. They are porous and consist of small crystalline particles whereas spray coated films show a densely packed columnar

structure [14]. Recent studies indicated that it is possible to improve the structure of sol-gel coatings by increasing the sintering temperature and the heating rate of the sintering process [15] using for example CO_2 laser densification [16, 17].The resistivity of the coatings depends also on the layer thickness. It sharply decreases with increasing total thickness up to a value of 200-300 nm. Therefore one way to improve the sheet resistance is to increase the total layer thickness by repeating the coating cycles [18].

In this paper we investigate the influence of the sintering conditions on the electrical and structural properties and on the chemical composition of SnO_2:Sb multilayers made by the sol-gel process.

EXPERIMENTAL

Multilayer sol-gel coatings have been deposited on borosilicate glass by dip coating using a 0.2 molar ethanolic solution of $SnCl_2(OAc)_2$ containing 5 mol% $SbCl_3$ in a controlled atmosphere (T=20°C, RH= 40 %). The densification of the coatings was performed by three different processes (Fig. 1) where each coating consisted of a different number of layers having the **same** total thickness about 250 nm in dry state. The thickness of the individual layers was adjusted by changing the withdrawal speed. It is worthwhile to note that for process I a drying stage at a temperature lower than 200°C (e.g. 120°C) leads to cracked layers. The final heat treatment was always realised by introducing the layers directly into a preheated furnace at 550°C.

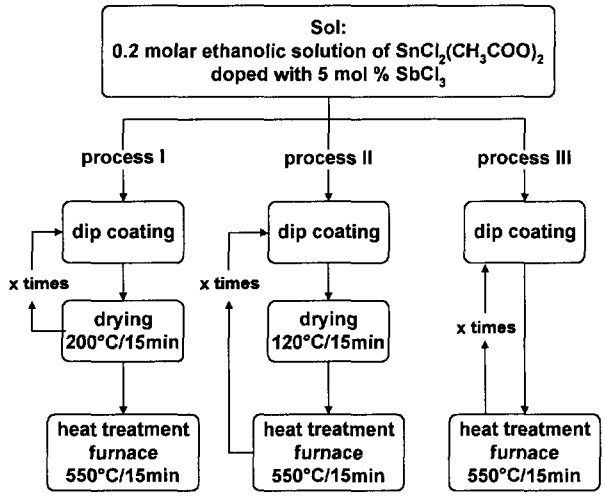

Fig. 1: Flow diagram of the various procedures

The layer thickness was determined by a surface profiler (Tencor P10). The electrical properties of the coatings were measured by the 4 probe method and the Van der Pauw/Hall technique (MMR Technology with a 1.5 T magnetic field). The texture has been observed by high resolution transmission microscopy and the crystallite size was determined from XRD spectra (Siemens D500). The chemical composition was investigated by Secondary Neutral Mass Spectrometry (SNMS) using a Leybold INA 3-equipment connected to a quadropole-mass spectrometer. The SNMS measurement were performed with a different batch of samples than the electrical measurements.

RESULTS AND DISCUSSION

The drying and sintering temperature influence the thickness of the multilayer. For example a multilayer coating prepared with 10 coating cycles with the **same** withdrawal speed and sintered according to process II or III has a total thickness of 180 nm while the same coating prepared according to process I has a total thickness of 232 nm. The total thickness for all multilayer coatings made according to process I

was always found about 25 % higher than the thickness of those obtained by the other processes, which hardly differ from each other. This can be explained by differences in the layer morphology as shown by the HRTEM cross sections. (Fig. 2 and Fig. 3). The multilayer coating made by process I is porous but homogeneous and built with small (6-8 nm) almost spherical crystallites that are loosely packed (Fig. 2). On the contrary, the morphology of the multilayers obtained according to process III reveals that each individual layer consists of a two layer structure: a thin 10 nm relatively dense interface lying on top of a more porous bulk layer (Fig. 3). The crystallite's size is about 6 nm. Because the multilayers made by processes II and III are equally thick it is assumed that the structure of the coating prepared by process II is also built of consecutive porous and dense layers. The morphologies of the multilayers is similar to that found for single layers sintered and heated in the same conditions [10].

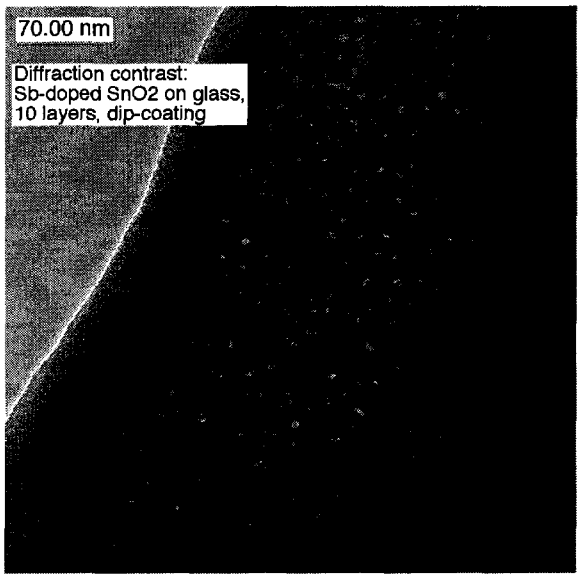

Fig. 2: HRTEM cross section of a 10 layers coating prepared according to process I

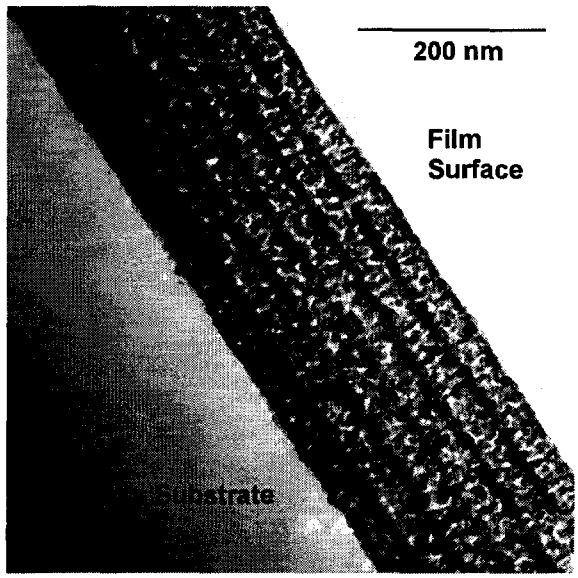

Fig. 3: HRTEM cross section of a 6 layers coating prepared according to process III

These different morphologies have a dramatic effect on the electrical parameters of the coatings. For multilayer coatings obtained by process I the resistivity is practically independent of the number of layers i.e. the resistivity is the same 1.4×10^{-2} Ωcm for a coating made of 4 x 58 nm or a 10 x 23.2 nm thick layers (Fig. 5). The electron mobility $\mu = 1,7$ cm²/Vs and the carrier density (electron) $N = 2,5 \times 10^{20}$ cm³ are also practically constant for each coating. A different behaviour has been found for coatings made by process II and III. In both cases the electrical properties are strongly dependent on the number of layers (Fig. 5). An increasing number of layers leads to a decrease of the resistivity from $\rho = 3,6 \times 10^{-3}$ Ωcm for a 4 x 45 nm thick coating to $\rho = 1.8 \times 10^{-3}$ Ωcm for a 10 x 18 nm thick coating. The electron mobility increases from $\mu = 2,93$ cm²/Vs for the 4 layers coating to $\mu = 4,5$ cm²/Vs for a 10 layers coating. However the carrier density remains constant $N = (4 \times 10^{20}$ cm$^{-3})$. A higher conductivity is therefore observed when the number of the dense interfaces increases. The thin layers should have consequently a lower resistivity than the internal part of each layers.

The resistivity ρ_e of the dense interfaces and the resistivity ρ_i ($\rho_i > \rho_e$) of the porous bulk can be determined by assuming that the sequence of the single layers is connected electrically in parallel (Fig. 4). In this case the macroscopic sheet resistance is given by the sum of the single layer sheet resistance. For a given multilayer built with n layers with alternating porous and dense regions, the macroscopic resistivity is given by:

$$\frac{1}{\rho_n} = \frac{1}{\rho_i} + \frac{d_e}{d}\left(\frac{1}{\rho_e} - \frac{1}{\rho_i}\right) \cdot n \qquad (1)$$

A plot of the measured resistivity of the multilayers made by the three processes versus the number of layers is shown in Fig. 5. For each process a straight line is obtained with almost equal intercept ~ 50 $(\Omega cm)^{-1}$. For process II and III the slope has nearly the same value of 22 $(\Omega cm)^{-1}$, while for process I the reciprocal resistivity is practically constant.

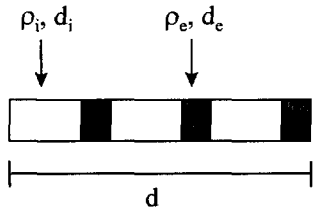

Fig. 4: Scheme of a 3 layer system with a total thickness d obtained by process II and III. The denser surface layer of thickness d_e is shaded.

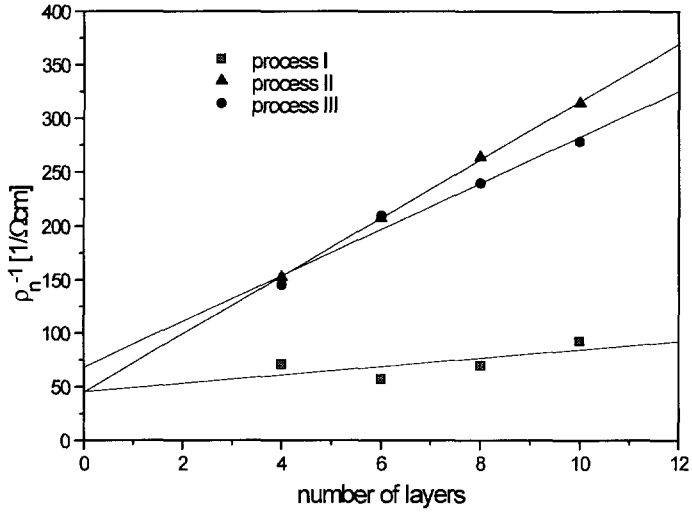

Fig. 5: Reciprocal of the measured resistivity ρ_{n-1} vs. the number of layers deposited. The straight lines are a fit accordingly to equation 1. The total thickness of each sintered coatings is 232 nm (Process I) and 180 nm (Process II and III).

The resistivity ρ_e of the dense interface of each layer was calculated assuming that the thickness of the dense interfaces measured from the HRTEM pictures was 10 nm (Table 1).

Table 1: Values of ρ_i and ρ_e calculated from (1) and Fig. 5 for coatings made according to process I, II, III.

Process	I	II	III
ρ_i (Ωcm)	0,014	0,014	0,014
ρ_e (Ωcm)	-	0,0018	0,0022

The chemical composition of the coatings (C, O, Si, Sn, Sb) and the ratio Sn:Sb was examined by SNMS for two 4 times dipped multilayers made by process I and process III respectively (Fig. 6 and Fig. 7). In both samples no carbon was detected and the surface shows an excess of O probably due to atmospheric water and OH-group absorbed after the obtention of the coatings.

For the multilayer coating produced by process I the depth profile of the ratio Sn:Sb is practically constant and corresponds to the composition of the sol. The Sn concentration slightly increases continuously toward the substrate while the O concentration has an opposite behaviour. Near the

substrate the ratio Sn:O corresponds practically to the SnO_2 composition. In this process the 4 layers where first dried at 200°C and at this stage considerable amount of organic materials are still included in the coating. During the sintering process at 550°C the organic material lying at the air/coating interface will react more strongly with the oxygen from air than the organic material lying deeper in the layer, which will mostly react with oxygen inside the coating.

When each layer is sintered at 550° C without a predrying step (process III) the shape of the concentration profile of Sn, O, Sb is totally different (Fig. 7). The oxygen concentration does not decrease in the direction to the substrate and the 4 sequential structures of the coating are clearly observed by the alternating maxima and minima for O, Sn and the ratio Sb:Sn. As the first minimum of this ratio lies at the layer's surface it is assumed that their minima correspond to the dense part of the multilayer and their maxima to the porous part of the layer. At the minima, the Sn:Sb ratio agrees with the value of the sol composition. The Sb and Sn concentration proceeds according to the Sn:Sb curve while the O concentration has an opposite behaviour. The composition of the dense and porous part is therefore different. As the amount of Sb is small compared to the amount of Sn the difference in the composition of the dense vs. bulk part of the layers is essentially related to change in Sn . In the dense interface the ratio Sn:O corresponds almost perfectly to the SnO_2 composition whereas in the porous structures the ratio Sn:O corresponds to a composition SnO_{2-x} with x> 0.5. In the porous part of the layer the Sb concentration is higher than in the dense part. More Sb seems necessary to keep the electrical neutrality of the layer, due probably to the higher surface of the particles (lower density).

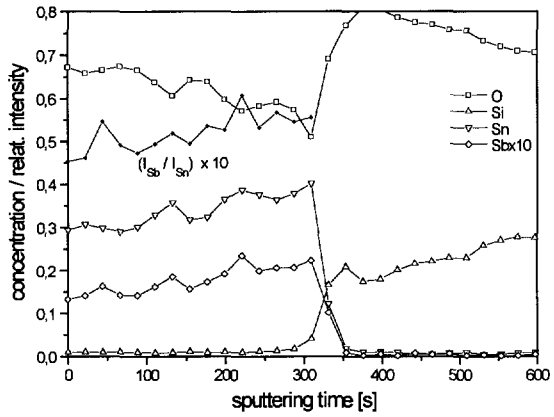

Fig. 6: SNMS of a 4 layers coating 187 nm thick prepared by process I

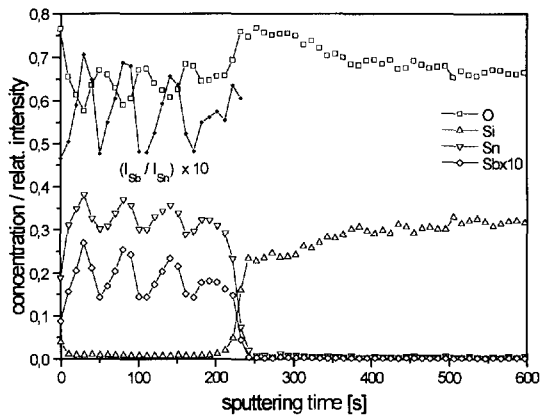

Fig. 7: SNMS of a 4 layers coating 230 nm thick prepared by process III

CONCLUSION

The influence of drying and sintering conditions on the electrical and morphological properties and the chemical composition profiles of sol gel SnO_2:Sb multilayers has been reported. Multilayers coating made of layers of same thickness, individually sintered in air at 550°C are composed of alternated layers consisting of a dense external layer on top of a porous bulk structure. A model was proposed to calculate the resistivity of the dense layer $\rho_e = 2{,}2 \times 10^{-3}$ Ωcm and the porous layer $\rho_i = 1{,}4 \times 10^{-2}$ Ωcm. The chemical composition of both layers is different. In the dense part the composition is nearly SnO_2 with a ratio Sb:Sn = 5 %. In the porous layer the composition corresponds to SnO_{2-x}, with x >0,5 and a ratio Sb:Sn = 7 %. For coating made with single layers all dried at 200°C and where the whole coating was then sintered at 550°C, the resistivity is independent of the number of layers and the final total thickness. The value is $\rho_2 = 1.4 \times 10^{-2}$ Ωcm. The morphology of the coating is homogenous as well as their chemical composition. It corresponds to SnO_2 with a ratio Sb:Sn = 5 %.

ACKNOWLEDGEMENTS

We are grateful to the Institut für Oberflächen and Schichtanalytik GmbH in Kaiserslautern, Germany, where the SNMS measurements were performed and to Dr. T. Krajewski for the TEM analysis. The financial support of the Bundesministerium für Bildung und Forschung (BMBF, Project 2A 67/03N0940) and the State of Saarland is gratefully acknowledged.

REFERENCES

[1] K.L. Chopra, S. Major and D.K. Pandya, "Transparent conductors - a status review", *Thin Solid Films,* 102 1-46 (1983).

[2] J. Dutta, P. Roubeau, T. Emeraud, J.-M. Laurent, A. Smith, F. Leblanc and J. Perrin, "Application of pyrosol deposition process for large-area deposition of fluorine-doped tin dioxide thin films", *Thin Solid Films,* 239 150-5 (1994).

[3] C.G. Grandquist, "Transparent conductive electrodes for electrocromic devices: A review", *Applied. Physics /A,* 57 19-24 (1993).

[4] C.G. Grandquist, "Window coatings for the future", *Thin Solid Films,* 193/194 730-41 (1990).

[5] L. Meng and M.P. dos Santos, "The effect of substrate temperature on the properties of sputtered tin oxide films", *Thin Solid Films,* 237 112-7 (1994).

[6] F.J. Yusta, M.L. Hitchman and S.H. Shamlian, "CVD preparation and characterization of tin dioxide films for electrochemical applications", *Journal of Materials Chemistry,* 7 1421-7 (1997).

[7] C.J.R. Gonzalez-Oliver and I. Kato, "Tin(antimony)-oxide sol-gel coatings on glass", *Journal of Non-Crystalline Solids,* 82 400-10 (1986).

[8] Y.J. Lin and C.J. Wu, "The Properties of antimony-doped tin oxide thin-films from the sol-gel process", Surface & Coatings Technology, 88 239-47 (1997).

[9] S.S. Park and J.D. Mackenzie, "Sol-gel-derived tin oxide thin-films", *Thin Solid Films,* 258 268-73 (1995).

[10] T.M. Racheva and G.W. Critchlow, "SnO_2 thin films prepared by the sol- gel process", *Thin Solid Films,* 292 299-302 (1997).

[11] T.D. Senguttuvan and L.K. Malhotra, "Sol-gel deposition of pure and antimony doped tin dioxide thin-films by non alkoxide precursors", *Thin Solid Films,* 289 22-8 (1996).

[12] Y. Takahashi and Y. Wada, "Dip-coating of Sb-doped SnO_2 films by ethanolamine-alkoxide method", *Journal of the Electrochemical Society,* 137 267-72 (1990).

[13] C. Terrier, J.P. Chatelon and J.A. Roger, "Electrical and optical-properties of Sb-SnO_2 thin-films obtained by the sol-gel method", *Thin Solid Films,* 295 95-100 (1997).

[14] M.A. Aegerter, A. Reich, G. Ganz, G. Gasparro and J. Pütz, "Comparative study of SnO_2:Sb transparent conducting films produced by various coating and heat treatment techniques", *Journal of Non-Crystalline Solids,* 218 123-9 (1997).

[15] J. Pütz, D. Ganz, G. Gasparro and M.A. Aegerter, "Influence of the heating rate on the microstructure and on macroscopic properties of sol-gel SnO_2:Sb coatings", *Journal of Sol-Gel Science and Technology,* accepted.

[16] G. Ganz, A. Reich and M.A. Aegerter, "Laser firing of transparent conducting SnO_2 sol-gel coatings", *Journal of Non-Crystalline Solids,* 218 242-7 (1997).

[17] D. Ganz and M.A. Aegerter, "Laser sintering of SnO_2:Sb sol-gel coatings", *Journal of Sol-Gel Science and Technology,* accepted.

[18] S.S. Park and J.D. Mackenzie, "Microstructure effects in multidipped tin oxide-films", *Journal of the American Ceramic Society,* 78 2669-72 (1995).